ACS APPLIED MATERIALS & INTERFACES

www.acsami.org Research Article

Melt Processable Novolac Cyanate Ester/Biphenyl Epoxy Copolymer Series with Ultrahigh Glass-Transition Temperature

Jiaxiong Li, Chao Ren, Zhijian Sun, Yanjuan Ren, Haksun Lee, Kyoung-sik Moon, and Ching-Ping Wong*

Cite This: https://doi.org/10.1021/acsami.0c20537 Read Online

ACCESS | Metrics & More | Article Recommendations

ABSTRACT: The rapid progress in silicon carbide (SiC)-based technology for high-power applications expects an increasing operation temperature (up to 250 °C) and awaits reliable packaging materials to unleash their full power. Epoxy-based encapsulant materials failed to provide satisfactory protection under such high temperatures due to the intrinsic weakness of epoxy resins, despite their unmatched good adhesion and processability. Herein, we report a series of copolymers made by melt blending novolac cyanate ester and tetramethylbiphenyl epoxy (NCE/EP) that have demonstrated much superior high-temperature stability over current epoxies. Benefited from the aromatic, rigid backbone and the highly functional nature of the monomers, the highest values achieved for the copolymers are as follows: glass-transition temperature (T_g) above 300 °C, decomposition onset above 400 °C, and char yield above 45% at 800 °C, which are among the highest of the known epoxy chemistry by far. Moreover, the high-temperature aging (250 °C) experiments showed much reduced mass loss of these copolymers compared to the traditional high-temperature epoxy and even the pure NCE in the long term by suppressing hydrolysis degradation mechanisms. The copolymer composition, i.e., NCE to EP ratio, has found to have profound impacts on the resin flowability, thermomechanical properties, moisture absorption, and dielectric properties, which are discussed in this paper with in-depth analysis on their structure−property relationships. The outstanding high-temperature stability, preferred and adjustable processability, and the dielectric properties of the reported NCE/EP copolymers will greatly stimulate further research to formulating robust epoxy molding compounds (EMCs) or underfill for packaging next-generation high-power electronics.

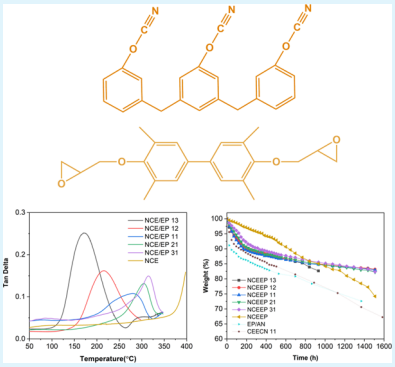

KEYWORDS: *epoxy, cyanate ester, copolymer, thermal stability, power electronics, encapsulant*

Downloaded via GEORGIA INST OF TECHNOLOGY on March 30, 2021 at 15:36:33 (UTC).
See https://pubs.acs.org/sharingguidelines for options on how to legitimately share published articles.

1. INTRODUCTION

Electric vehicles (EVs) and hybrid electric vehicles (HEVs) continue to strive in the global automotive markets as to tackle the stringent needs of seeking alternative energy sources and reducing CO_2 emissions.[1] As key power electronic components in these electricity driven cars, converter and inverter technologies used in drivetrain and charging systems (for plug-in HEV) are exerting to boost the efficiency of power transmission.[2,3] Higher power density and further miniaturization of these electronic devices are called for to achieve the above-mentioned goals in the drivetrain electrification. The next-generation wide-band-gap (WBG) semiconductors, namely, silicon carbide (SiC) and gallium nitride (GaN) will be the driving force to bring about revolutionary changes, with their capabilities far exceeding the silicon technology by supporting high-voltage/temperature operation, fast switch characteristics, and superior thermal conductivity.[4]

Packaging the WBG chips has, however, become a grand challenge and, in fact, the bottleneck to exploit the full potential of these chips at the desired operation temperature (250 °C for future SiC).[5] Of these components, the encapsulant, such as an epoxy molding compound (EMC), underfill and glob top, is one of the key enablers for long-term package reliability. It protects the chip and interconnects against dust, moisture, chemicals, and mechanical stresses from both internally and the environment.[6] Compared to the traditional silicone gel sealing, the fast-adopted molded power cards encapsulated by EMC offer advantages including modular design, compacted form factor, and the ability to inject mold-complicated structures in three-dimensional (3D) packages or double-sided cooling modules.[7,8] Though tremendous progresses in epoxy and epoxy composite technologies have been seen in the recent years,[9−11] typical epoxy (EP) resins could not withstand a continuous operation at a temperature above 150 °C, even with higher end products

Received: November 17, 2020
Accepted: March 15, 2021

 © XXXX American Chemical Society

with higher aromaticity in backbones and higher cross-link densities.[6,12] Their low glass-transition temperatures (T_g) expose the high coefficient of thermal expansion (CTE) to other substrates, generating interfacial stress that could lead to failure. Furthermore, the resins suffer from degradation and further decompose under high heat for a prolonged period, which severely deteriorate the physical and mechanical properties of EMCs that are crucial to protect the package.

Novel moldable epoxy chemistry showing enhanced thermal stability is therefore highly desired to formulate reliable EMC materials under such high operation temperatures. Blending, or preferably copolymerizing, with other high-temperature polymers has been proven to be a very useful method to improve the heat resistance of epoxy. Polyimide,[13,14] bismaleimide,[15,16] and cyanate ester (CE)[17,18] are some of the candidates that have drawn widespread attention for this use. CE makes use of the cyclotrimerization of cyanate groups to form aromatic triazine rings in situ, providing a superior thermal stability in the cured resin.[18] The relatively large free volume and low polarity of the cured resin further endow preferred dielectric properties, i.e., low dielectric constant and loss, for high-frequency applications. More importantly, the mature knowledge of copolymer chemistry on CE and epoxy offers the greater freedom of handling the copolymers of both.

The early works demonstrating the CE and epoxy compounds can be dated back to the early 1970s from Mitsubishi Gas Chemical Co., where they synthesized bismaleimde/triazine (BT) resin for high-temperature substrate applications,[19] although the product suffered from severe blistering due to impure CE monomers. Since then, a great deal of interest was shared by both academia and industries to acquire the understanding of the CE/epoxy copolymer chemistry and to synthesize satisfactory resins for various applications. Extensive works done by Shimp,[20,21] Ising,[22,23] Bauer and Bauer,[24−26] and Hamerton[27−29] have laid solid foundations and paved the way for us to utilize the fascinating properties of CE/EP copolymers with desired processability and high-temperature performances. Aiming at enhancing the high-temperature stability of epoxy for EMC applications in power packages, we have been thoroughly investigating selected CE/EP systems to gather information including their intrinsic properties and degradation pattern under high-temperature aging conditions.[30−32] Counterintuitively, the high T_g formulations with rich CE feeds normally experienced larger weight losses and severe blistering in the aging studies. In our previous work, the hydrolysis degradation of cyanate groups and decomposition of carbamates were identified to be responsible for this premature failure in these resins. The unsatisfactory high-temperature aging stability of the current CE/EP system motivates further exploration into high-performance monomers; to name one, the novolac type CE monomers that are known to support excellent high-temperature properties.

In this work, we report an extremely high heat-resistant novolac CE/tetramethylbiphenyl epoxy (NCE/EP) copolymer series with varied compositions. The thermomechanical and thermal properties of the polymer were examined through thermomechanical analysis (TMA), dynamic mechanical analysis (DMA), and thermal gravimetric analysis (TGA), revealing the increasing trend of both T_g (up to 300 °C) and decomposition onset $T_{10\%}$ (above 400 °C) and char yield (CR) with increasing NCE ratios. The addition of epoxy, on the other hand, rendered control over the flowability of the uncured resin, which is critical in handling compounding and injection molding of EMCs. The dielectric properties and the moisture absorption kinetics of the resin have also been analyzed and discussed in detail. During the long-term high-temperature (250 °C) aging, all copolymer samples exhibited similar weight loss behavior that significantly outperformed the typical epoxy-anhydride chemistry and our previous bisphenol A CE/EP systems. Other changes in the properties including CTE, T_g, and decomposition of these aged samples are also reported and compared. The encouraging results from this study recommend the NCE/EP copolymer resin as a promising candidate to prompt future research and applications in packaging future high-power devices.

2. EXPERIMENTAL SECTION

2.1. Materials. Primaset PT-30 cyanate ester resin (NCE) was supplied by Lonza AG (Basel, Switzerland). Tetramethylbiphenyl epoxy (TMBP) with an epoxide equivalent weight of 197 was supplied by Mitsubishi Chemical Corporation (Tokyo, Japan). Copper(II) acetylacetonate (Cu(II) acac, >99.99%) and nonylphenol (technical grade) were purchased from Aldrich. The reagents were used as received.

The chemical structures of the NCE, TMBP, and the Cu(II) acac catalyst are shown in Figure 1.

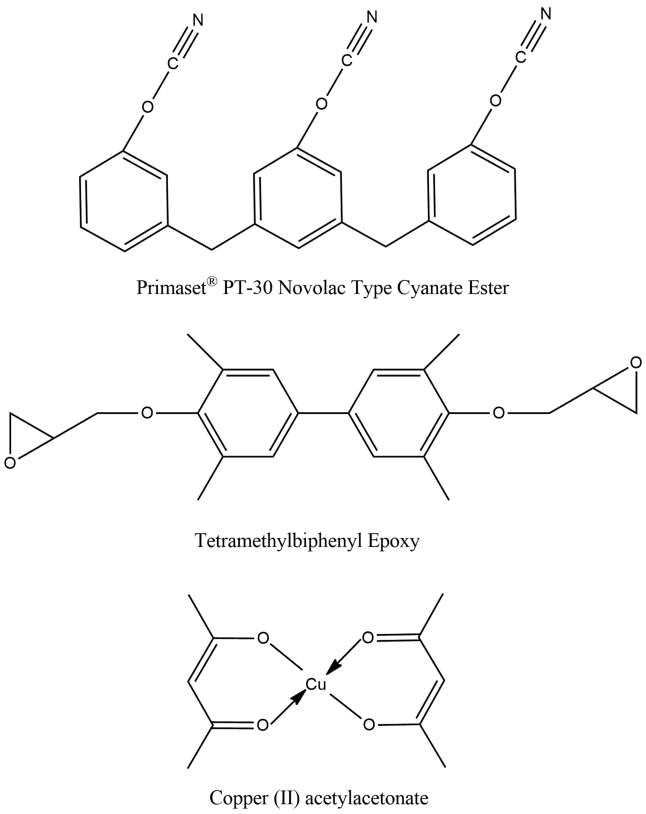

Figure 1. Chemical structures of Primaset PT-30 cyanate ester resin (NCE), tetramethylbiphenyl epoxy, and copper(II) acetylacetonate.

2.2. Preparation of NCE/EP Copolymer Samples. All of the polymer blends were based on the molar ratio between cyanate groups from NCE and epoxide groups (i.e., NCE/EP 13 represents formulation with cyanate/epoxide of 1:3 molar ratio). In this work, five different NCE/EP copolymer compositions ranging from 1:3 to 3:1 molar ratio (namely 1:3, 1:2, 1:1, 2:1, and 3:1) were investigated. The monomers were melted at 130 °C with magnetic stirring in an aluminum weighing pan (28 mm diameter). The catalyst Cu(II) acac

https://doi.org/10.1021/acsami.0c20537
ACS Appl. Mater. Interfaces XXXX, XXX, XXX−XXX

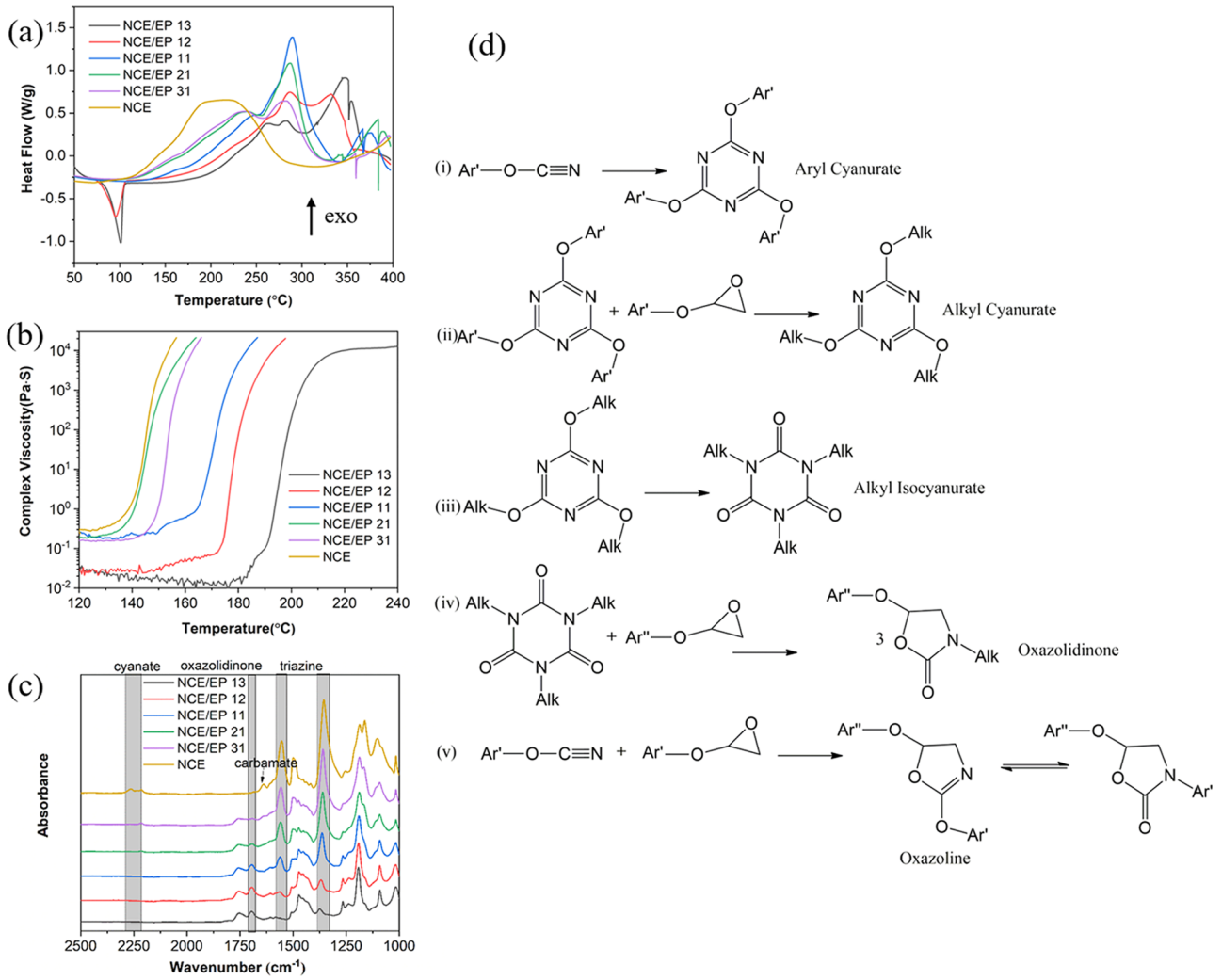

Figure 2. (a) DSC thermogram, (b) viscosity during temperature increase of NCE and NCE/EP monomer blends, (c) FTIR spectra of cured NCE and NCE/EP copolymers, and (d) main chemical reactions within the CE/EP system[21] (reproduced with permission from ref 21 Copyright 1995, Elsevier).

and the cocatalyst nonylphenol were premixed at a desired ratio and added drop wise into the monomer melt at a concentration of 360 ppm of Cu(II) ions and 3 phr (parts per hundred resin) of nonylphenol to the NCE resin. The curing schedule of the samples was 2 h at 150 °C, 2 h at 200 °C, and 3 h at 250 °C, with an increasing rate of 10 °C/min in between the stages, in a convection oven. A control high-temperature epoxy sample was made by blending ESCN 195XL resin (ECN) (Sumitomo Chemical, Tokyo, Japan) with methylhexahydrophthalic anhydride hardener (Lindride 52D, Lindau Chemicals Inc., Columbia) at a 1:0.85 weight ratio and cured for 2 h at 150 °C followed by 2 h at 200 °C. The final cured disk-shaped samples were polished for aging tests and cut into desired dimensions for thermomechanical tests.

2.3. Characterization. Differential scanning calorimetry (DSC) was performed at an increasing rate of 10 °C/min from 40 to 350 °C under a 50 mL/min nitrogen flow (DSC Q2000, TA Instruments, New Castle). In each scan, approximately 10 mg of the sample was encapsulated in aluminum sealed pans without piercing. Rheological properties of the polymer were tested by a hybrid rheometer by increasing at 10 °C/min from 120 to 240 °C or until the complex viscosity reached 20 000 Pa·S (Discovery HR-2, TA Instruments, New Castle). Thermal mechanical analysis (TMA) was performed at an increasing rate of 20 °C/min from 40 to 300 °C under a 50 mL/min nitrogen flow (TMA Q400, TA Instruments, New Castle) with an expansion probe. The TMA samples were prepared by cutting the cured resins to a size of 10 mm × 10 mm × 1 mm. Dynamic mechanical analysis (DMA) was performed in a tension mode with the film dimension at 10 mm × 8 mm × 1 mm, with an increased rate of 3 °C/min from 40 to 300 °C in an air atmosphere at an oscillation frequency of 1 Hz (DMA Q800, TA Instruments, New Castle). The thermal gravimetric analysis (TGA) tests were programmed to increase at 20 °C/min from 40 to 800 °C under a 50 mL/min nitrogen flow (TGA Q50, TA Instruments, New Castle) using approximately 10 mg of the sample in platinum Q50 pans. The same decomposition weight profile under an air atmosphere (100 mL/min) increased again at 20 °C/min from 40 to 800 °C was obtained from a Simultaneous DSC ad TGA (SDT Q600, TA Instrument, New Castle) with 10 mg of sample in an alumina pan. The disk-shaped samples with 28 mm diameter and approximately 1 mm thickness were used in all of the following tests. Dielectric permittivity and loss of the samples were scanned from 1 MHz to 1 GHz (E4991A RF Impedance Analyzer, Agilent, Santa Clara) at room temperature. Fourier-transform infrared spectroscopy (FTIR) was performed using a diamond attenuated total reflectance (ATR) mode (Nicolet iS5 FT-IR spectrometer, Thermo Scientific, Waltham) with a resolution of 4 cm^{-1} from 500 to 3500 cm^{-1}, and 64 scans were done for each sample. An in situ FTIR measurement to track down the chemical structure evolutions during cure was carried out on samples quenched at a desired temperature with an increase rate of 10 °C/min. The moisture absorption measurement was performed at 85 °C/85 relative humidity (RH) atmosphere (MicroClimate bench top environmental chamber, Cincinnati SubZero Inc., Cincinnati); the

https://doi.org/10.1021/acsami.0c20537
ACS Appl. Mater. Interfaces XXXX, XXX, XXX−XXX

samples were taken out at different time intervals to measure the weight gain. The high-temperature aging test was performed at 250 °C in circulating air (825f convection oven, Fisher Scientific, Waltham) where weight loss, chemical structure, and thermomechanical properties of the samples over aging time as well as the chemical structure change were recorded.

3. RESULTS AND DISCUSSION

3.1. Curing Behavior of NCE/EP Copolymers. The curing behavior of the copolymers was analyzed by both DSC and rheological studies, and is shown in Figure 2a,b, respectively. In the presence of a Cu^{2+} catalyst, the exotherm onset of pure NCE was suppressed to as low as 120 °C. For the copolymers, a rather diffracted pattern was shown while generally two major peaks could be found. First of all, when increasing the epoxy concentration, the melting occurred at below 100 °C, which is inherited from the tetramethylbiphenyl epoxy and which is in solid form at room temperature. At the same time, the onset of the low-temperature peak shifted upward, while the area underneath it decreased. The opposite trend was noticed for the second curing exotherm. Based on our previous work and the results documented in the literature,[25,32,33] it could be identified that the low-temperature exotherm represents the cyclotrimerization reactions of CE (Figure 2d,i), where the higher EP feed ratios diluted such reactants, while the copolymerization between CE and EP needs to be triggered at a further increased temperature where such peaks become evident in the EP-rich formulations.

The viscosity of the copolymers and their gel behavior during curing is shown in Figure 2b. The low viscosity of the epoxy monomers is crucial for the compounding process in producing EMC pellets or liquid-type EMCs, as a loading level of above 90 wt % of silica has become the general trend to render the ultra-low CTE properties in these EMCs to handle warpage issues at the wafer level and low profile advanced packaging.[34,35] In addition, the flowability of the compound during injection molding is a key parameter to be considered for evenly distributed void-less encapsulation in fine pitch applications, where highly flowable base resins are favored to compensate the appreciable viscosity increase due to the reduction in the filler size. In this system, a rather low complex viscosity of less than 0.1 Pa·s was observed in the pure NCE heated to 120 °C. With the incorporation of epoxy, which functions as a diluting agent,[36] the viscosity of the monomers was further gradually reduced to a level below 0.01 Pa·s. These intriguing features suggest that these polymer blends are ideal for processing heavily loaded compounds, owing to the fact that their flowability could be adjusted through composition control. The gel behavior of the copolymers agreed well with the curing thermogram. The viscosity of the mixture gradually increased upon heating and a dramatic increase was observed that leads to the gel point, which marks the degree of cure where the infinite cross-linked network structure is constructed. This viscosity buildup occurred at roughly the same temperature of the onset of the first exothermic peak in DSC plots for each formulation, where higher epoxy concentrations introduced a larger processing temperature window.

The chemical structures of the cured polymers could be interpreted from the FTIR spectra in Figure 2c. A clear trend of increasing triazine (1543 and 1360 cm^{-1}) content was evidenced when increasing the NCE feed ratio in the blend, along with the decrease of the copolymerization product oxazolidinone (1743 cm^{-1}) content. In other words, and quite intuitively, the cured resins from NCE-rich formulations are dominated by triazine structures, while those with high epoxy concentrations present stronger copolymer characteristics. The rigid and highly aromatic triazine structures endow the high T_g and good heat-resistant properties in the high NCE formulations, as evidenced in the thermomechanical properties presented in the following section. It is, however, worth noticing that after the curing at 250 °C for 3 h, pure NCE was still not fully cured with the evidence of remaining doublet peaks of cyanate groups at 2250 cm^{-1}. The multifunctional nature and the closely packed novolac structure of the NCE have increased the difficulty in fully consuming the cyanate groups, where the cyclotrimerization requires three cyanate groups to be gathered together, especially in the diffusion-controlled curing stage when the T_g of the resin surpasses the curing temperature. At the same time, prolonged high temperature holding for further cure could bring in concurrent high-temperature degradation issues. In fact, the standing out carbonyl groups at ∼1690 cm^{-1} could be attributed to the carbamate formation from cyanate groups.[37] This carbamate decomposes at over 190 °C to release CO_2 gas,[21] which could cause blistering problems in the product. This competition between further cure and decomposition at the same time creates the dilemma of higher temperature or longer time cures. By introducing epoxy monomers in the system, full conversion of the cyanate groups was achieved, as they provide an alternative path in consuming these cyanate groups. This fact would account for the enhanced high-temperature aging stabilities of the copolymers discussed in the later section.

3.2. Thermomechanical Properties of NCE/EP Copolymers. The thermomechanical properties of the NCE/EP blends were investigated by various characterizations. The results from TMA tests are listed in Table 1. The CTE of the cured resin is a vital parameter, as its mismatch with those of the silicon, substrate, or solder joints is the source of accumulated thermal stress during molding and thermal cycling, which could lead to severe warpage or interfacial delamination/crack issues.[38] A combination of low CTE and high T_g of epoxy resin is favored for EMC application, as for high T_g resins, less or no portion of α_2 CTE (usually several times higher than α_1 CTE) is exposed to the operation temperature. In this system, the T_g of the copolymer determined by TMA increased linearly with NCE portions in the feed, from 161.0 to 272.5 °C with the cyanate to epoxide ratio ranging from 1:3 to 3:1. The NCE/EP 21 and 31 formulations showed a T_g higher than 250 °C, which is higher than most harsh environments in consumer or automotive applications. The α_1 CTE of the resins were within typical ranges around 60 ppm/K, while the α_2 CTE displayed a general trend of first decreasing and then increasing values along the NCE concentration. This CTE variation of a

Table 1. Parameters from TMA Tests on NCE/EP Copolymers Including the T_g and CTE before (α_1) and after (α_2) Glass Transition

NCE/EP	TMA T_g/°C	α_1/ppm/°C	α_2/ppm/°C
13	161.0	65.4	528.0
12	220.5	69.3	238.7
11	226.6	75.2	355.2
21	251.0	52.8	133.5
31	272.5	50.9	193.9

https://doi.org/10.1021/acsami.0c20537
ACS Appl. Mater. Interfaces XXXX, XXX, XXX−XXX

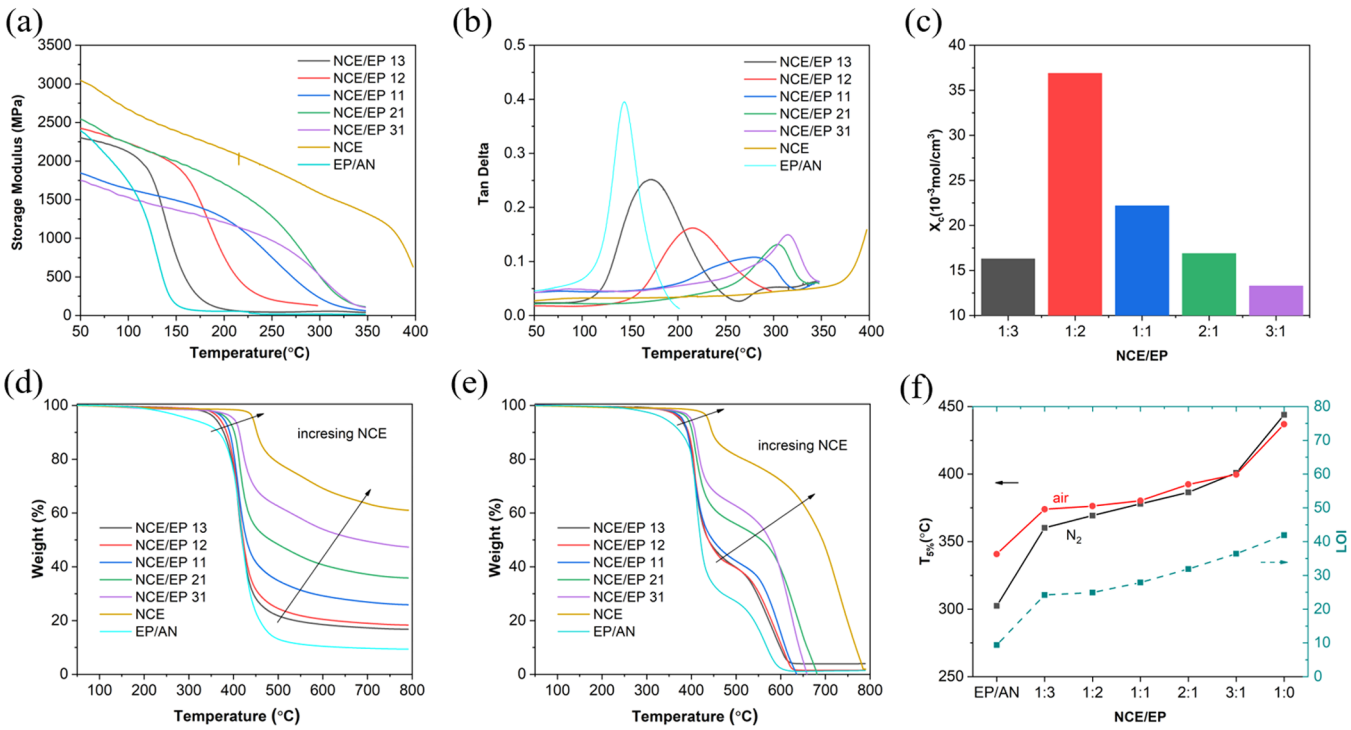

Figure 3. DMA (a) storage modulus and (b) tan δ profile; (c) estimated cross-link density (X_c) from rubbery modulus; TGA weight loss profile in (d) N_2 and (e) in air; and (f) temperature at 5% weight loss ($T_{5\%}$) and limited oxygen index (LOI) of cured NCE and NCE/EP copolymers.

rubberized resin at above T_g implies the cross-link density difference, where by increasing the content of NCE in the formulation, the cross-link density initially increased and then decreased. The introduction of NCE initially in the epoxy offered more cross-linking sites, while for high NCE formulations, the dominant trimerization reaction (that requires three cyanate groups at each cross-linking knot) over copolymerization inevitably reduced the cross-link density, presenting the more CE-like characteristic.

Thermal stability of the copolymer system is further evaluated through DMA and TGA. Figure 3a shows the storage modulus of the copolymers, where with increase in the NCE ratio, the modulus before glass transition first increased and then decreased, in line with the cross-link density trend in TMA. Figure 3b shows the tan δ profiles of the NCE/EP copolymers from the DMA test to capture T_g of the material from the DMA test. The parameters extracted from the DMA test including T_g and storage modulus in the rubbery state, used to calculate the cross-link density, are listed in Table 2. An extraordinary T_g of above 400 °C was obtained for the pure NCE polymer, benefited from the high aromaticity. Similar to the TMA results, the T_g of the NCE/EP copolymer from the DMA test showed a linear increasing trend when increasing the NCE content in the system, with the lowest already reaching above 170 °C. The high T_g values for all formulations is a combination result of the rigid building blocks from both monomers and the cross-link points, which are both sterically hindered for relaxation. A T_g of above 300 °C from the DMA test was successfully obtained in the blend system for NCE/EP 21 and 31, significantly higher than those of the traditional epoxy materials (epoxy/anhydride as a reference in Figure 3 and Table 2), and the previously reported CE/EP systems struggle to achieve 250 °C.[12,17,30,32,36,39−43] Also, in line with the observed α_2 CTE of the copolymers series, the same trend of cross-link density was observed in the DMA studies, first from the area under the tan δ peaks. The damping properties imply the internal molecular restraints when the polymer experiences glass transition, and that polymers with lower cross-link density present more lossy characteristics, i.e., a larger out-of-phase component (loss tangent) in the strain/stress responses. In this system, a first decreasing and then increasing trend of the peak area was captured when increasing the NCE concentrations in the feed, suggesting the exact opposite trend of the cross-link density. A more detailed estimation of cross-link density was given by the analysis of storage modulus of the polymer in its rubbery region[44−46] as

$$X_c = \frac{E'}{3RT'} \tag{1}$$

where X_c is the estimated cross-link density, E' is the storage modulus in the rubbery region (at 30 °C higher than T_g), R is the ideal gas constant (R = 8.314 J/(mol·K)), and $T' = T_g + 30$ °C. The calculated results are shown in Figure 3c and listed in the last column of Table 2. The same trend again supports the conclusion from TMA studies and the discussions on the damping properties. The initial increase in cross-link density

Table 2. DMA Thermomechanical Properties of NCE/EP Copolymers, Including T_g, Storage Moduli at Rubbery Region, and the Calculated Cross-Link Density

NCE/EP	DMA T_g/°C	E' at 30 °C above T_g/MPa	cross-link density/10^{-3} mol/cm^3
EP/AN	144.0	63.4	14.6
13	170.1	81.6	16.3
12	214.2	224.8	36.9
11	278.0	170.6	22.2
21	305.8	141.3	16.9
31	314.8	114.3	13.3

https://doi.org/10.1021/acsami.0c20537
ACS Appl. Mater. Interfaces XXXX, XXX, XXX−XXX

from the epoxy-dominant formulations should be related to the additional reaction mechanisms from NCE to the ring opening of epoxides. The highest cross-link density appeared at a medium NCE concentration, and further increase of the NCE content resulted in the loss of cross-link density as in cured CE.

The thermal decomposition behavior of these copolymers is monitored by TGA, shown in Figure 3d,e, with parameters subtracted from the curves summarized in Table 3. The temperature at 5% weight loss ($T_{5\%}$) and the estimated limited oxygen index value are plotted against NCE content in Figure 3f for better illustration. As shown in Figure 3d,f, once again, the copolymer resin showcased a much-improved thermal stability compared to the epoxy/anhydride formulation, and a linear positive correlation of decomposition temperature and NCE concentration was found, where for NCE/EP 31 formulation, the 5% weight loss temperature remarkably achieved 400 °C in both N_2 and air, with the latter one being representative for the real applications in oxidative environments. In these environments, in addition to the typical chain scission and radical formation when approaching the decomposition limit, oxygen brings about the formation of peroxide radicals that are highly unstable and easily transferred, accelerating the degradation process. However, these effects are not significant in our systems, as the decomposition onset in air is similar, in fact slightly higher, to that in N_2 for many formulations. The onset weight loss is still thermodynamically governed by the bond energy of the weakest links to the evaporable components. The rapid coupling of the peroxide radicals may even introduce further vitrification, thereby elevating the breakdown temperature. The novolac building blocks and the formed triazine structures in the NCE-rich copolymers were credible for the enhancement of thermal robustness of the copolymer network, postponing the decomposition onset via both the presence of bulky thermal stable repeating units and the restrained diffusion/radical transfer in these high T_g resins lacking chain mobilities.[47] In addition, the residue weight of these polymers after decomposition in N_2 (above 60 wt % remaining at 800 °C for NCE) is also quite eye-catching, and high char yield is known to be beneficial for flame retardance properties, which are crucial for EMC to protect electronic devices under fire environments. It also became quite clear that in the second stage of weight loss in air (the burning of char, at above the decomposition limit of around 450 °C), the high NCE formulations demonstrated the greatly enhanced flame

Table 3. Summarized Parameters from TGA Thermogram of the NCE/EP Blends, Including the Temperature at 5 and 10% Weight Loss, Residue Weight at 800 °C (Char Yield), and Estimated Limited Oxygen Index (LOI)

NCE/EP	$T_{5\%}$ in N_2/°C	$T_{10\%}$ in N_2/°C	$T_{5\%}$ in air/°C	$T_{10\%}$ in air/°C	char yield at 800 °C in N_2/%	LOI
EP/AN	302.4	365.4	340.8	376.8	9.4	21.3
13	360.2	378.1	374.0	391.8	16.8	24.2
12	369.3	384.7	376.3	393.6	18.4	24.9
11	378.0	391.5	380.3	391.0	25.9	27.9
21	386.5	402.0	392.4	402.2	35.9	31.9
31	400.9	413.0	399.7	408.4	47.3	36.4
10	443.9	452.5	436.9	446.7	61.0	41.9

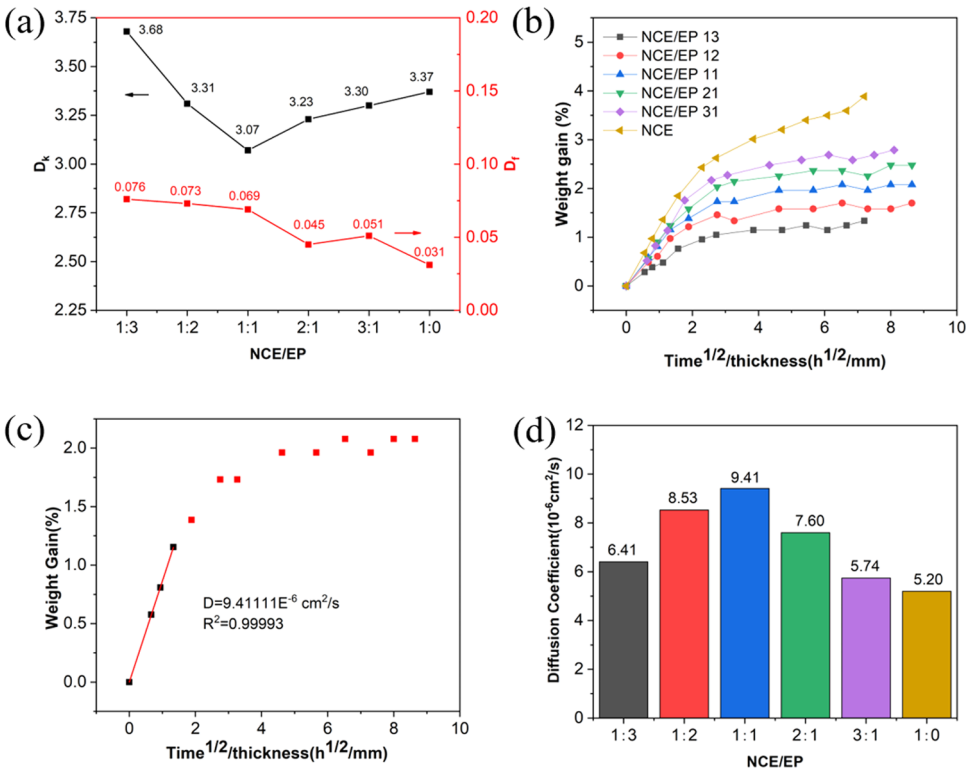

Figure 4. (a) Dielectric constant (D_k) and loss tangent (D_f) at 10 MHz, (b) moisture absorption of the NCE and NCE/EP copolymers under the 85 °C/85 RH condition, (c) example of analysis of the initial diffusion-controlled phase of moisture uptake in NCE/EP 11 under the 85 °C/85 RH condition, and (d) summarized diffusion coefficients of moisture ingression in the NCE and NCE/EP copolymers under the 85 °C/85 RH condition.

https://doi.org/10.1021/acsami.0c20537
ACS Appl. Mater. Interfaces XXXX, XXX, XXX−XXX

retardancy by the largely delayed weight drop. As a quantitative evaluation, limited oxygen index (LOI) was defined as the minimum oxygen concentration to support the combustion of a polymer under a certain gas environment. Quite naturally, high LOI denotes the retardancy of the polymer against ignition. An empirical equation gives the estimate of LOI based on char yield (CR) in N_2 from TGA data[48]

$$\mathrm{LOI} = 17.5 + 0.4\mathrm{CR} \tag{2}$$

The calculated values are listed in the last column in Table 3 and more clearly plotted in Figure 3f. Very high LOI from 24.2 to greater than 40 was presented in the system, which is actually higher than most epoxy systems with specially designed flame retardants.[49,50] To be more specific, the LOI categorizes the polymer as follows: LOI $\leq$ 20.95, flammable; 20.95 $\leq$ LOI $\leq$ 26, marginally stable; and LOI $\geq$ 26, self-extinguishable.[48] The continuous increase of LOI in the copolymer based on the NCE content ranged from at least marginally stable to the highly self-extinguishable behavior in the formulations with higher than 1:1 cyanate/epoxide ratio. The highly aromatic nature of the copolymers helped in developing the characteristic of a strong char-forming tendency, leaving rich carbonaceous residues after elimination of oxygen and hydrogen atoms when heated or ignited. These structures impede the diffusion of both oxygen and flammable volatiles in burning conditions, thereby presenting the superior flame retardance behavior that qualifies them for electronic packing applications in extreme environments.

3.3. Dielectric Properties and Moisture Absorption Kinetics of NCE/EP Copolymers. Dielectric properties of the copolymers and their moisture absorption behavior under the 85 °C/85 RH condition are plotted in Figure 4a,b, respectively. Not only are these parameters essential for EMC applications—where the dielectric properties impact the signal delay and transmission loss[51] and moisture absorption greatly influences the package reliability during solder reflow, thermal shock, or thermal cycling conditions where the escaping vapor causes cracking or bubbling ("popcorn crack")[52]—but also they together provide useful insights into the internal material structures. When increasing the NCE concentration, the D_k initially decreased until it reached a 1:1 ratio, where further charging NCE monomers in the feed caused a reversed effect in D_k. The D_k represents the internal dielectric response (polarization) of the polymer under the field. The epoxy-rich formulations provided abundant polar −OH sites to orient when the field is applied, resulting in high D_k in these resins. Increasing the NCE ratio, as we have discussed in the previous section, would provide alternative curing routes to reduce the overall polarity, plus an increase in the cross-link density, which restrains the chain motion. These merits contributed to the favored low D_k properties in the NCE/EP 12 and 11 resins. On further increasing the NCE content, as the cross-link density instead decreased, the enhanced chain mobility and large free volume allowed the rotation and alignment motions for the polar groups, which is why one may find the increasing trend of D_k in these later formulations. Regarding D_f, first, the reduction in population of polar −OH groups relieved the force applied on polymer chains under the field; second, the later creation of the larger free volume and the loosely cross-linked structure in the high NCE resins caused rather free rotations of these chains from restraints/frictions (which causes the phase lag and heat generation, and therefore, the loss). A continuous decrease of D_f along NCE ratios is therefore expected based on the combination of these two effects.

The moisture absorption curves in Figure 4b revealed a clear trend of increasing water uptake in the final equilibrium stage with NCE concentrations, which is in line with the findings of Karad et al.[53] The value ranged from 1 wt % for NCE/EP 13 sample to up to over 4 wt % in pure NCE. The gradual emergence of coordination sites for water molecules, for example the triazine rings,[54] and the remaining cyanate moieties prone to hydrolysis[55] in these high NCE end of the copolymer series have likely outweighed the effects of resin polarity, as discussed in the last section. A careful selection of resin formulation is, therefore, to be made when formulating the EMC materials based on moisture sensitivity of the application.

For the first time, a deeper investigation of the moisture ingression kinetics in CE/EP copolymers was performed. During the initial stage of wet conditioning, the water uptake of the polymer disk sample follows precisely a simplified Fick's law, giving a linear relationship when plotted against $t^{1/2}/h$ (time$^{1/2}$/thickness),[56] as

$$\frac{M_t}{M_\infty} = \frac{4}{h}\sqrt{\frac{Dt}{\pi}} \tag{3}$$

where M_t is the moisture uptake at time t, M_∞ is the moisture uptake at equilibrium, and D is the diffusion coefficient. The fitting (with the example for NCE/EP 11 shown in Figure 4c) showed good linear correlation and solved the diffusion coefficient for each formulation, as shown in Figure 4d. Interestingly, the D presented a first increasing and then decreasing trend against the NCE content, exactly opposite to the trends of cross-link density and D_k. The penetration of moisture in the resin depends on both the driving force, the polar−polar interaction of certain groups with water,[57] and the availability of channeling paths, i.e., the free volume in the molecular structure. In light of the geometrical considerations, one may naturally speculate that higher cross-link networks impose greater steric hindrances for moisture transport. Though this may hold true in many cases, where the loosely cross-linked structure with high chain mobility resists poorly to moisture diffusion,[54] experimental facts are not rare to present a reversed trend,[58,59] where water diffuses faster in highly cross-linked polymers as in our case. In this reported NCE/EP copolymer system, we would postulate that the strong affinity between water and the cross-link site, including hydroxyl groups, oxazolidinone,[60] and triazine, could in fact present these linkages as hosts for water molecules[61] that facilitate the hopping of them in the cross-linked network. This would be an interesting discovery and further work should be pursued to gain better understandings of this phenomenon.

3.4. High-Temperature Aging Analysis of NCE/EP Copolymers. The high-temperature aging stability of resins is yet another determining factor for employing them in high-power applications. Polymers, regardless of their initial properties, degrade over time under continuous exposure to increased temperature. Thermo-oxidative degradation is a major concern in most thermoset materials, where the chain scission under applied heat was facilitated by the formation of peroxyl radicals. The reactive chain end then propagates, which is eventually terminated by coupling (further vitrification) or disproportionation (decreased molecular weight and formation

https://doi.org/10.1021/acsami.0c20537
ACS Appl. Mater. Interfaces XXXX, XXX, XXX−XXX

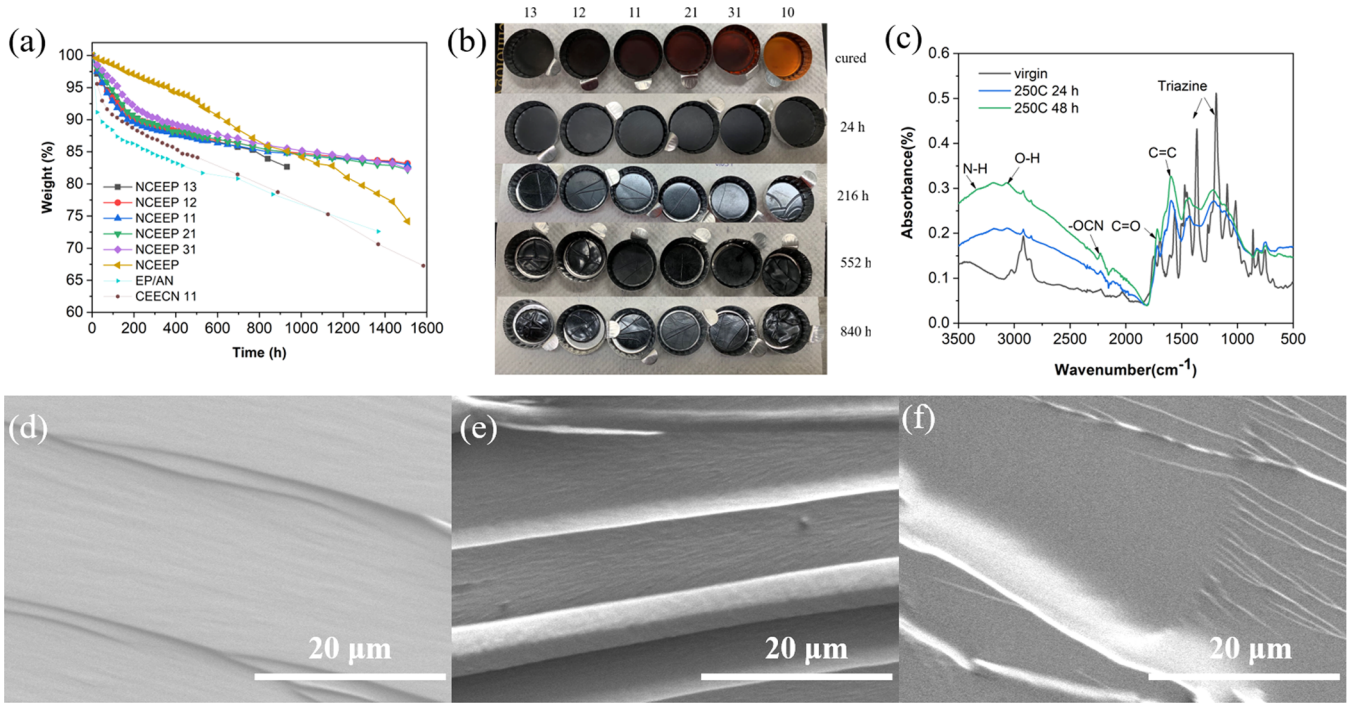

Figure 5. (a) Weight loss of NCE/EP copolymers, a typical epoxy/anhydride (EP/AN) formulation and a CE/epoxidized cresol novolac (ECN) formulation (reproduced with permission from ref 32 Copyright 2020, Elsevier) under 250 °C aging; (b) images of NCE/EP copolymers during 250 °C aging at different time intervals; (c) FTIR spectra of virgin NCE/EP 11 sample and that aged under 250 °C for 24 and 48 h; and scanning electron microscopy (SEM) images of (d) virgin fractured NCE/EP 11 surface that aged under 250 °C for (e) 8 h and (f) 24 h.

of an unsaturated structure). The integrity of epoxy compounds against such harsh environments dictates the final reliability of the encapsulated product. The weight loss of these organic materials during aging at 250 °C was taken as the measuring merit and is plotted versus time in Figure 5a. As a comparison, the data of a typical high-temperature formulation with epoxy cured by anhydride and a previous CE/EP system are supplied here as well. All of the copolymer formulations described in this work presented a similar weight loss trend, while it is clear that their high-temperature handling capability greatly surpasses that of the traditional high-temperature epoxy or the bisphenol A type CE/EP blends. As mentioned, the reduced weight loss in these samples is the result of the highly rigid backbone structure (including the novolac and the tetramethylbiphenyl molecules) imposing kinetic restraints for the diffusion of oxygen, the propagation of the radicals, as well as the escaping of volatile chain-scission products. Quite naturally, the formulations with higher T_g and decomposition onset experienced less weight loss over the course of aging. Moreover, these copolymer formulations have stabilizing effects on the NCE homopolymer in prolonged high-temperature storage. Even though the pure NCE exhibited an outstanding heat resistance during the initial 700 h, further exposure to 250 °C caused its fast, almost linear with time, degradation, with a severely swollen/distorted morphology. Also, despite the superior TGA char yields of pure NCE, the high-temperature aging continuously broke down the resins leading to an even greater weight loss compared to the copolymer series, which distinctively exposes its alternative degradation mechanism from the short-term decomposition. From the discussions in previous sections and the known knowledge of hydrolysis degradation of CE, the appreciable remaining cyanate groups in the network and the greater moisture absorption in pure NCE likely contribute to the carbamate formation and decomposition reactions to release CO_2 gas,[21,62] while the copolymers suppressed these reactions by consuming the majority of free cyanate groups. The copolymers in the high NCE ends, still, akin to the NCE polymer, inevitably suffered from larger weight loss eventually through this mechanism despite their witnessed robustness in the short term. The increase of cyanate (2250 cm^{-1}) intensity observed might have resulted from the decyclization of triazine (1543 and 1360 cm^{-1}),[63] and the amine (3360 cm^{-1}) indicating carbamate formation. A quite obvious turning point in the weight loss rate of these copolymers is found at roughly 250 h. In the initial aging stage, the −OH rich resins typically go through dehydration reaction that results in an unsaturated structure (see the emerging signal for C═C (1585 cm^{-1}) in Figure 5c, and the darkening of sample color), and the oxidative reactions causing chain scission at relatively weak points (the large increase of O−H (3070 cm^{-1}) intensity in Figure 5c) indicate the scission at ether linkages forming free hydroxyl groups, presenting reactive radical at chain ends. The rapid release of water and easier evaporation of short-chain segments result in the observed weight loss, while the coupling of the radicals at chain ends gradually turned the resin into a shrunk, densely cross-linked, carbon-dominated structure (also suggested by the microcracks in Figure 5e,f that represent the brittleness of the resin), eventually to what is often referred to as char (see the deep aged samples in Figure 5b). The slow diffusion and oxidation of this carbonaceous phase would account for the observed much reduced decomposition rate in the later aging stage after the initial 250 h. Again, with the mature knowledge of the CE/EP degradation mechanism in mind (thermo-oxidative degradation and the hydrolysis degradation of cyanate groups), the major advancement in the formed copolymer series over the conventional epoxy and previously reported CE/EP resins is based on its highly

https://doi.org/10.1021/acsami.0c20537
ACS Appl. Mater. Interfaces XXXX, XXX, XXX−XXX

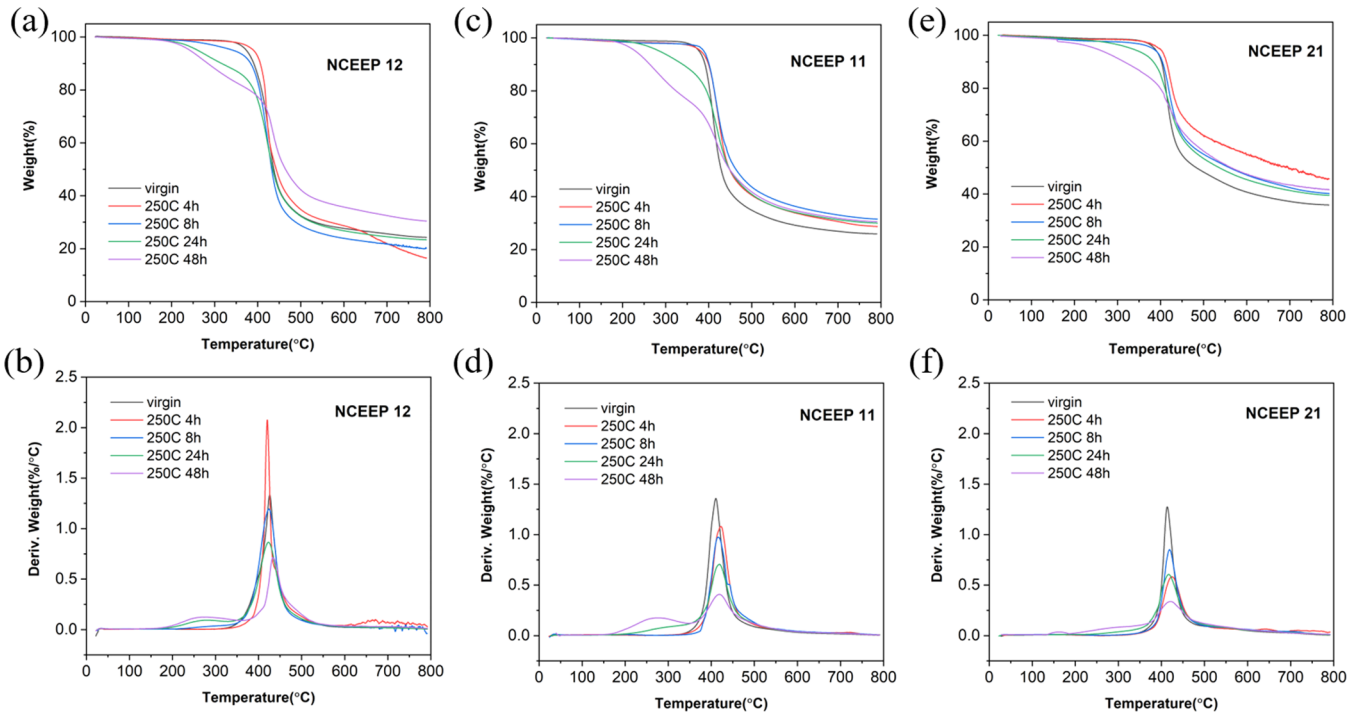

Figure 6. TGA and DTG thermograms of NCE/EP copolymers in N_2 during 250 °C aging. (a, b) NCE/EP 12; (c, d) NCE/EP 11; and (e, f) NCE/EP 21.

functionalized and aromatic monomer structures, i.e., novolac and tetramethylbiphenyl, and the in situ formation of rigid triazine rings. The high rigidity (kinetically) and stability (chemically and therefore thermodynamically) of these building blocks contribute to the remarkable high T_g and decomposition temperature, which promotes the high-temperature aging behavior in a similar manner.

To gain further understandings of the internal structure change during this degradation process, the thermal decomposition results of the aged and unaged samples are compared. As the far NCE or the far EP end of the copolymer series experienced larger weight loss and premature failure during high-temperature aging (likely due to the loosely cross-linked structure as discussed in DMA studies), the medium formulations such as NCE/EP 12, 11, and 21 are selected in the scope of degradation studies. Their TGA and DTG profiles along aging at 250 °C for up to 48 h are shown in Figure 6. The slightly improved thermal resistance was shared by all three compositions after the short-term aging within 8 h. This was the result from the further vitrification of the resin, sterically restricting the thermal decomposition. Both further curing and the coupling of radicals would contribute to this densification effect. In addition, certain unstable weight may have already been removed from the system during aging. During prolonged holding of the samples at high temperature, a remarkable early breakdown behavior can be spotted at near 200 °C. Especially, the emerging weight loss peak in the DTG diagram of NCE/EP 11 (Figure 6d) clearly shows the trend of gradual development in this phenomena. It can thus be inferred that in this stage, the samples are filled with abundant easily breakable bonds, and the molecules are free to be evaporated. In particular, eliminated water from the dehydration reaction is likely the major product, as supported by the darkened look of the samples due to double bond formation, accompanied by methane or aldehyde type molecules from chain scission and rearrangements.[64] The highly aromatic and closely packed structure with very few weak linkages in these resins should resist the release of main chain components at such low temperature. Again, the quite high char yield of these aged samples was attributed to this high aromaticity, which was not harmed by the high-temperature storage. Nevertheless, the presence of this low-temperature decomposition peak (with onset below 200 °C) is in correlation with the rather fast weight loss kinetics in the early stages of 250 °C aging, shown in Figure 5a. In the higher NCE ratio copolymers, for instance the NCE/EP 12, the apparent flattening of this peak also marks its stronger robustness against the thermal decomposition during oxidative aging.

The evolution of thermomechanical properties, which are vital for the encapsulant reliability, of the resin during aging was examined and further insights into the degradation pattern were provided. Through the plasticization effect of moisture[65] and the oxidative degradation inside the resin, the T_g normally decreases upon high-temperature storage. Table 4 lists the results of TMA tests on the aged NCE/EP samples, again with 12, 11, and 21 formulations. A clear trend of the decreasing T_g value in all samples was found along with aging time. Looking into more details, for the low NCE formulation, i.e., NCE/EP 12, one shall find the remarkable shrinking of α_2 CTE after 4 h of aging. This denotes that further cross-linking had occurred due to either curing reaction or recombination of radicals, which is in good agreement with the observed higher decomposition onset of this sample in Figure 6a. Although NCE/EP 11 suffered from the most severe T_g regression and CTE increase after 48 h of aging (as is for the prominent low-temperature weight loss peak in TGA), further introduction of aromatic and bulky NCE molecules in the system supported a better integrity in maintaining the high T_g for the NCE/EP 21 composition. Again, note the greatly suppressed CTE values of

https://doi.org/10.1021/acsami.0c20537
ACS Appl. Mater. Interfaces XXXX, XXX, XXX−XXX

Table 4. Parameters from TMA Tests on NCE/EP Blends during Aging under 250 °C Aging Including the T_g and CTE before (α_1) and after (α_2) Glass Transition

NCE/EP	aging time/h	TMA T_g/°C	α_1/ppm/°C	α_2/ppm/°C
1:2	0	220.5	69.3	238.7
	4	187.3	61.9	207.1
	8	157.9	60.9	230.6
	24	155.8	44.2	208.2
	48	151.3	78.5	396.8
1:1	0	226.6	75.2	355.2
	4	208.8	62.3	196.2
	8	188.4	60.4	391.9
	24	166.2	95.9	416.5
	48	123.8	102.5	280.0
2:1	0	251.0	52.8	133.5
	4	211.1	46.3	138.4
	8	210.4	59.9	175.0
	24	187.8	65.9	218.8
	48	162.3	67.5	230.5

the 4 h aged NCE/EP 21 sample; this should suggest the occurrence of further cross-linking in the systems, which supported the greatly enhanced thermal stability of this product under TGA increase (Figure 6e). Overall, it could be concluded that in the short-term high-temperature aging, the higher NCE ratio formulations such as NCE/EP 21 present the most attracting stabilities needed for EMC to protect the package, while even higher NCE ratios may, from Figure 5a, suffer from greater weight loss in the long term due to unfavored hydrolysis degradation.

4. CONCLUSIONS

This study presents a novel NCE/EP-based copolymer series that show great potential for high-temperature epoxy encapsulation applications. Thanks to the extremely high aromaticity of the NCE monomer, a remarkable T_g (over 300 °C) and decomposition onset ($T_{5\%}$ over 400 °C) were achieved for the epoxy-based copolymers, and these merits were associated with the evident lower mass loss during 250 °C aging far superior to the bisphenol A CE/EP blends and traditional anhydride-cured high-temperature epoxies, even the pure NCE in the long term as severe hydrolysis strikes in the latter polymer. The resin flowability, thermomechanical properties, and dielectric properties were found controllable by altering the copolymer composition (NCE to EP ratio), and the competing effects of aromaticity, cross-link density, and polarity in each formulation were analyzed and discussed in detail to account for these interesting behaviors. The high-temperature aging experiments not only recognized their enhanced reliability but also provided knowledge on the degradation processes in different copolymer formulations by tracking the decomposition and thermomechanical properties of the aged samples. In summary, copolymerizing NCE and EP provides a series of products with great high temperature robustness, melt processability, and dielectric properties that made them attractive for formulating high-temperature stable epoxy compounds to encapsulate future WBG power devices. We would also anticipate that specific applications benefited from individually selected resin compositions to meet their unique processing or operation needs.

AUTHOR INFORMATION

Corresponding Author

Ching-Ping Wong − *School of Materials Science and Engineering, Georgia Institute of Technology, Atlanta, Georgia 30332, United States;* orcid.org/0000-0003-3556-8053; Email: cp.wong@mse.gatech.edu

Authors

Jiaxiong Li − *School of Materials Science and Engineering, Georgia Institute of Technology, Atlanta, Georgia 30332, United States*

Chao Ren − *School of Biological and Chemical Engineering, Anhui Polytechnic University, Wuhu, Anhui 241000, China*

Zhijian Sun − *School of Materials Science and Engineering, Georgia Institute of Technology, Atlanta, Georgia 30332, United States*

Yanjuan Ren − *Department of Materials Science and Engineering, CAPT/HEDPS/LTCS, Key Laboratory of Polymer Chemistry and Physics of Ministry of Education, College of Engineering, Peking University, Beijing 100871, China*

Haksun Lee − *School of Electrical and Computing Engineering, Georgia Institute of Technology, Atlanta, Georgia 30332, United States*

Kyoung-sik Moon − *School of Materials Science and Engineering, Georgia Institute of Technology, Atlanta, Georgia 30332, United States*

Complete contact information is available at: https://pubs.acs.org/10.1021/acsami.0c20537

Notes

The authors declare no competing financial interest.

ACKNOWLEDGMENTS

This work was supported by the Industry Consortium at the Georgia Tech Packaging Research Center (PRC). The gratis sample of Primaset PT-30 cyanate ester resin from Lonza AG and the help from Roger Mazotti and Delane Tomlinson are appreciated. This work was performed in part at the Georgia Tech Institute for Electronics and Nanotechnology, a member of the National Nanotechnology Coordinated Infrastructure (NNCI), which is supported by the National Science Foundation (Grant ECCS-2025462).

REFERENCES

(1) Das, H.; Rahman, M.; Li, S.; Tan, C. Electric Vehicles Standards, Charging Infrastructure, and Impact on Grid Integration: A Technological Review. *Renewable Sustainable Energy Rev.* **2020**, *120*, No. 109618.

(2) Feng, S.; Magee, C. L. Technological Development of Key Domains in Electric Vehicles: Improvement Rates, Technology Trajectories and Key Assignees. *Appl. Energy* **2020**, *260*, No. 114264.

(3) Emadi, A.; Lee, Y. J.; Rajashekara, K. Power Electronics and Motor Drives in Electric, Hybrid Electric, and Plug-in Hybrid Electric Vehicles. *IEEE Trans. Ind. Electron.* **2008**, *55*, 2237−2245.

(4) Roccaforte, F.; Fiorenza, P.; Greco, G.; Nigro, R. L.; Giannazzo, F.; Iucolano, F.; Saggio, M. Emerging Trends in Wide Band Gap Semiconductors (Sic and Gan) Technology for Power Devices. *Microelectron. Eng.* **2018**, *187−188*, 66−77.

(5) Lee, H.; Smet, V.; Tummala, R. A Review of Sic Power Module Packaging Technologies: Challenges, Advances, and Emerging Issues. *IEEE J. Emerging Sel. Top. Power Electron.* **2020**, *8*, 239−255.

(6) Komori, S.; Sakamoto, Y. Development Trend of Epoxy Molding Compound for Encapsulating Semiconductor Chips. In *Materials for Advanced Packaging*; Springer, 2009; pp 339−363.
(7) Lu, M.-C. Comparative Study on Power Module Architectures for Modularity and Scalability. *J. Electron. Packag.* **2020**, *142*, No. 040801.
(8) Reimers, J.; Dorn-Gomba, L.; Mak, C.; Emadi, A. Automotive Traction Inverters: Current Status and Future Trends. *IEEE Trans. Veh. Technol.* **2019**, *68*, 3337−3350.
(9) Zhang, Z.; Du, Y.; Zhu, C.; Guo, L.; Lu, Y.; Yu, J.; Parkin, I. P.; Zhao, J.; Guo, D. Unprecedented Enhancement of Wear Resistance for Epoxy-Resin Graphene Composites. *Nanoscale* **2021**, *13*, 2855−2867.
(10) Meng, F.; Zhang, Z.; Gao, P.; Kang, R.; Boyjoo, Y.; Yu, J.; Liu, T. Excellent Tribological Properties of Epoxy—Ti3c2 with Three-Dimensional Nanosheets Composites. *Friction* **2020**, 1−13.
(11) Guo, L.; Zhang, Z.; Li, M.; Kang, R.; Chen, Y.; Song, G.; Han, S.-T.; Lin, C.-T.; Jiang, N.; Yu, J. Extremely High Thermal Conductivity of Carbon Fiber/Epoxy with Synergistic Effect of Mxenes by Freeze-Drying. *Compos. Commun.* **2020**, *19*, 134−141.
(12) Yao, Y.; Lu, G.-Q.; Boroyevich, D.; Ngo, K. D. Survey of High-Temperature Polymeric Encapsulants for Power Electronics Packaging. *IEEE Trans. Compon., Packag., Manuf. Technol.* **2015**, *5*, 168−181.
(13) Biolley, N.; Pascal, T.; Sillion, B. Polyimide-Modified Epoxy System: Time-Temperature-Transformation Diagrams, Mechanical and Thermal Properties. *Polymer* **1994**, *35*, 558−564.
(14) Qu, C.; Li, X.; Yang, Z.; Zhang, X.; Wang, T.; Wang, Q.; Chen, S. Damping, Thermal, and Mechanical Performances of a Novel Semi-Interpenetrating Polymer Networks Based on Polyimide/Epoxy. *J. Appl. Polym. Sci.* **2019**, *136*, 48032.
(15) Iredale, R. J.; Ward, C.; Hamerton, I. Modern Advances in Bismaleimide Resin Technology: A 21st Century Perspective on the Chemistry of Addition Polyimides. *Prog. Polym. Sci.* **2017**, *69*, 1−21.
(16) Xiong, X.; Chen, P.; Ren, R.; Lu, F.; Yu, Q. Cure Mechanism and Thermal Properties of the Phthalide-Containing Bismaleimide/Epoxy System. *Thermochim. Acta* **2013**, *559*, 52−58.
(17) Kim, B. S. Effect of Cyanate Ester on the Cure Behavior and Thermal Stability of Epoxy Resin. *J. Appl. Polym. Sci.* **1997**, *65*, 85−90.
(18) Hamerton, I. *Chemistry and Technology of Cyanate Ester Resins*; Springer Science & Business Media, 2012.
(19) Gaku, M.; Suzuki, K.; Nakamichi, K. Curable Resin Compositions of Cyanate Esters. U.S. Patent US4,110,3641978.
(20) Shimp, D.; Christenson, J.; Ising, S. In *Cyanate Esters−an Emerging Family of VersatileComposite Resins*, Proceedings of the 34th Annual International SAMPE Symposium, 1989; pp 222−233.
(21) Fang, T.; Shimp, D. A. Polycyanate Esters: Science and Applications. *Prog. Polym. Sci.* **1995**, *20*, 61−118.
(22) Shimp, D. A.; Ising, S. J. Flame Retardant Polycyanate Ester Blend.U.S.Patent US4,931,545A1990.
(23) Shimp, D.; Christenson, J.; Ising, S. *Arocy Cyanate Ester Resins: Chemistry, Properties and Applications*; Rhone-Poulenc: Louisville, KY, 1991.
(24) Bauer, J.; Bauer, M. Statistical Structural Model for the Gelation Behaviour of Cyanate-Epoxy Polyreactions. *Acta Polym.* **1988**, *39*, 548−551.
(25) Bauer, M.; Bauer, J. Networks from Cyanic Acid Esters and Glycidyl Ethers. *Makromol. Chem., Macromol. Symp.* **1989**, *30*, 1−11.
(26) Bauer, J.; Bauer, M. Kinetic Structural Model for the Network Build-up During the Reaction of Cyanic Acid Esters with Glycidyl Ethers. *J. Macromol. Sci., Part A: Chem.* **1990**, *27*, 97−116.
(27) Hamerton, I. High-Performance Thermoset−Thermoset Polymer Blends: A Review of the Chemistry of Cyanate Ester−Bismaleimide Blends. *High Perform. Polym.* **1996**, *8*, 83−95.
(28) Hamerton, I.; Hay, J. N. Recent Technological Developments in Cyanate Ester Resins. *High Perform. Polym.* **1998**, *10*, 163−174.
(29) Hamerton, I.; Hay, J. N. Recent Developments in the Chemistry of Cyanate Esters. *Polym. Int.* **1998**, *47*, 465−473.
(30) Wu, F.; Tuan, C.-C.; Song, B.; Moon, K.-S.; Wong, C.-P. Controlled Synthesis and Evaluation of Cyanate Ester/Epoxy Copolymer System for High Temperature Molding Compounds. *J. Polym. Sci., Part A: Polym. Chem.* **2018**, *56*, 1337−1345.
(31) Li, J.; Ren, C.; Moon, K.-s.; Wong, C.-p. In *Epoxy/Triazine Copolymer Resin System for High Temperature Encapsulant Applications*, 2019 IEEE 69th Electronic Components and Technology Conference (ECTC); IEEE, 2019; pp 2296−2301.
(32) Li, J.; Ren, C.; An, D.; Ren, Y.; Moon, K.-s.; Wong, C.-p. Systematic Evaluation of Cyanate Ester/Epoxidized Cresol Novolac Copolymer Resin System for High Temperature Power Electronic Packaging Applications. *Polymer* **2020**, *195*, No. 122454.
(33) Walters, R. N.; Lyon, R. E. Fire-Resistant Cyanate Ester−Epoxy Blends. *Fire Mater.* **2003**, *27*, 183−194.
(34) Oi, Y.; Fujii, Y.; Hiraoka, T.; Yada, Y.; Kan, K. In *Warpage Control of Liquid Molding Compound for Fan-out Wafer Level Packaging*, IEEE 68th Electronic Components andTechnology Conference (ECTC); IEEE, 2018; pp 967−972.
(35) Jeong, H.; Jung, K.-H.; Lee, C.-J.; Min, K. D.; Jung, S.-B. *Thermomechanical Properties of Fan-out Wafer Level Package Fabricated with Various Epoxy Mold Compound*, 22nd European Microelectronics and Packaging Conference & Exhibition (EMPC), IEEE: 2019; pp 1−5.
(36) Liang, G.; Zhang, M. Enhancement of Processability of Cyanate Ester Resin Via Copolymerization with Epoxy Resin. *J. Appl. Polym. Sci.* **2002**, *85*, 2377−2381.
(37) Pinchas, S.; Ben-Ishai, D. The Carbonyl Absorption of Carbamates and 2-Oxazolidones in the Infrared Region. *J. Am. Chem. Soc.* **1957**, *79*, 4099−4104.
(38) Shin, D. K.; Lee, J. J. Effective Material Properties and Thermal Stress Analysis of Epoxy Molding Compound in Electronic Packaging. *IEEE Trans. Compon., Packag., Manuf. Technol., Part B* **1998**, *21*, 413−421.
(39) Wang, C. S.; Lee, M. C. Synthesis, Characterization, and Properties of Multifunctional Naphthalene-Containing Epoxy Resins Cured with Cyanate Ester. *J. Appl. Polym. Sci.* **1999**, *73*, 1611−1622.
(40) Rakesh, S.; Dharan, C. P. S.; Selladurai, M.; Sudha, V.; Sundararajan, P. R.; Sarojadevi, M. Thermal and Mechanical Properties of Poss-Cyanate Ester/Epoxy Nanocomposites. *High Perform. Polym.* **2013**, *25*, 87−96.
(41) Liu, W.; Qiu, Q.; Wang, J.; Huo, Z.; Sun, H. Curing Kinetics and Properties of Epoxy Resin−Fluorenyl Diamine Systems. *Polymer* **2008**, *49*, 4399−4405.
(42) Pan, G.; Du, Z.; Zhang, C.; Li, C.; Yang, X.; Li, H. Synthesis, Characterization, and Properties of Novel Novolac Epoxy Resin Containing Naphthalene Moiety. *Polymer* **2007**, *48*, 3686−3693.
(43) Ren, H.; Sun, J.; Wu, B.; Zhou, Q. Synthesis and Characterization of a Novel Epoxy Resin Containing Naphthyl/Dicyclopentadiene Moieties and Its Cured Polymer. *Polymer* **2006**, *47*, 8309−8316.
(44) Chen, J.-S.; Ober, C. K.; Poliks, M. D.; Zhang, Y.; Wiesner, U.; Cohen, C. Controlled Degradation of Epoxy Networks: Analysis of Crosslink Density and Glass Transition Temperature Changes in Thermally Reworkable Thermosets. *Polymer* **2004**, *45*, 1939−1950.
(45) Levita, G.; De Petris, S.; Marchetti, A.; Lazzeri, A. Crosslink Density and Fracture Toughness of Epoxy Resins. *J. Mater. Sci.* **1991**, *26*, 2348−2352.
(46) Loren, W. H. *Dynamic Mechanical and Tensile Properties Paint and Coating Testing Manual: 15th. Edition of the Gardner-Sward Handbook*; ASTM International: West Conshohocken, PA, 2012; pp 624−636.
(47) Levchik, S. V.; Weil, E. D. Thermal Decomposition, Combustion and Flame-Retardancy of Epoxy Resins—a Review of the Recent Literature. *Polym. Int.* **2004**, *53*, 1901−1929.
(48) Venkatesh, M.; Gouthaman, S.; Kanemoto, S. O.; Lakshmi, M. S.; Hamerton, I. Development of Epoxy-Cyanate Ester-Clay Nanocomposites Offering Enhanced Thermally Stability. *J. Appl. Polym. Sci.* **2019**, *136*, 47754.

https://doi.org/10.1021/acsami.0c20537
ACS Appl. Mater. Interfaces XXXX, XXX, XXX−XXX

(49) Liu, Y. L.; Wu, C. S.; Hsu, K. Y.; Chang, T. C. Flame-Retardant Epoxy Resins from O-Cresol Novolac Epoxy Cured with a Phosphorus-Containing Aralkyl Novolac. *J. Polym. Sci., Part A: Polym. Chem.* **2002**, *40*, 2329−2339.
(50) Wang, X.; Song, L.; Xing, W.; Lu, H.; Hu, Y. A Effective Flame Retardant for Epoxy Resins Based on Poly (Dopo Substituted Dihydroxyl Phenyl Pentaerythritol Diphosphonate). *Mater. Chem. Phys.* **2011**, *125*, 536−541.
(51) Abe, S.; Mitsukura, K.; Imazu, Y.; Toba, M.; Masuko, T.; Kurafuchi, K. In *Low Dk and Df Photosensitive Insulation Material for Low Transmission Loss Packages*, International Symposium on Microelectronics, International Microelectronics Assembly and Packaging Society; International Microelectronics Assembly and Packaging Society, 2018; pp 415−418.
(52) Placette, M. D.; Fan, X.; Zhao, J.-H.; Edwards, D. Dual Stage Modeling of Moisture Absorption and Desorption in Epoxy Mold Compounds. *Microelectron. Reliab.* **2012**, *52*, 1401−1408.
(53) Karad, S. K.; Attwood, D.; Jones, F. R. Moisture Absorption by Cyanate Ester Modified Epoxy Resin Matrices. Part Iii. Effect of Blend Composition. *Composites, Part A* **2002**, *33*, 1665−1675.
(54) Georjon, O.; Galy, J. Effects of Crosslink Density on the Volumetric Properties of High Tg Polycyanurate Networks. Consequences on Moisture Absorption. *Polymer* **1998**, *39*, 339−345.
(55) Marella, V. V.; Throckmorton, J. A.; Palmese, G. R. Hydrolytic Degradation of Highly Crosslinked Polyaromatic Cyanate Ester Resins. *Polym. Degrad. Stab.* **2014**, *104*, 104−111.
(56) Li, L.; Zhang, S.; Chen, Y.; Liu, M.; Ding, Y.; Luo, X.; Pu, Z.; Zhou, W.; Li, S. Water Transportation in Epoxy Resin. *Chem. Mater.* **2005**, *17*, 839−845.
(57) Musto, P.; Ragosta, G.; Mascia, L. Vibrational Spectroscopy Evidence for the Dual Nature of Water Sorbed into Epoxy Resins. *Chem. Mater.* **2000**, *12*, 1331−1341.
(58) Diamant, Y.; Marom, G.; Broutman, L. J. The Effect of Network Structure on Moisture Absorption of Epoxy Resins. *J. Appl. Polym. Sci.* **1981**, *26*, 3015−3025.
(59) Barton, J. M. Effect of Absorbed Water on the Thermal Relaxation of Biaxially Stretched Crosslinked Poly (Methyl Methacrylate). *Polymer* **1979**, *20*, 1018−1024.
(60) Walles, W. E.; Tousignant, W. F. Water-Soluble Copolymers of Ring Substituted N-Vinyl-2-Oxazolidinone. U.S. Patent US2,948,7081960.
(61) Moy, P.; Karasz, F. E. Epoxy-Water Interactions. *Polym. Eng. Sci.* **1980**, *20*, 315−319.
(62) Kasehagen, L. J.; Haury, I.; Macosko, C. W.; Shimp, D. A. Hydrolysis and Blistering of Cyanate Ester Networks. *J. Appl. Polym. Sci.* **1997**, *64*, 107−113.
(63) Ramirez, M. L.; Walters, R.; Lyon, R. E.; Savitski, E. P. Thermal Decomposition of Cyanate Ester Resins. *Polym. Degrad. Stab.* **2002**, *78*, 73−82.
(64) Lee, L.-H. Mechanisms of Thermal Degradation of Phenolic Condensation Polymers. Ii. Thermal Stability and Degradation Schemes of Epoxy Resins. *J. Polym. Sci., Part A: Gen. Pap.* **1965**, *3*, 859−882.
(65) Ellis, T.; Karasz, F. Interaction of Epoxy Resins with Water: The Depression of Glass Transition Temperature. *Polymer* **1984**, *25*, 664−669.

https://doi.org/10.1021/acsami.0c20537
ACS Appl. Mater. Interfaces XXXX, XXX, XXX−XXX